QUANTIFIED PH IMAGING WITH HYPERPOLARIZED ^{13}C-BICARBONATE

David Johannes Scholz[1], Martin A. Janich[2], Annette Frank[3], Ulrich Köllisch[1], Jan H. Ardenkjaer-Larsen[4,5], Rolf F. Schulte[2], Markus Schwaiger[3], Axel Haase[1], and Marion I. Menzel[2]

[1]*IMETUM, Technische Universität München, Munich, Germany,* [2]*GE Global Research, Munich, Germany,* [3]*Nuclear Medicine, Technische Universität München, Munich, Germany,* [4]*Technical University of Denmark, Copenhagen, Denmark,* [5]*GE Healthcare, Copenhagen, Denmark*

Introduction: As pH plays a crucial role in several diseases, such as cancer but also hypoxia, inflammation etc., it is desirable to detect pH *in vivo*. Ideally, the detection should be noninvasive and spatially localized. A clinical tool for pH mapping is not yet available, despite the clinical impact, but a proof of concept was performed using hyperpolarized ^{13}C-Bicarbonate (^{13}C-BiC)[1]. To apply this promising method of pH detection to different diseases, it is important to quantify and compare it to already established methods of pH detection.
In this work, pH mapping was quantified *in vitro* focusing on method-based errors originating from hardware, chemical and biological uncertainties. pH mapping with spectral-spatial (SPSP) excitation[2] and spiral readout was applied *in vivo* on healthy rats and animals with induced metabolic alkalosis and with acute inflammation.

Methods: *In vitro* quantification was partly performed with ^{13}C-Na-BiC (Sigma Aldrich). ^{13}C-Cs-BiC was synthesized with enriched $^{13}CO_2$ gas and subsequently prepared to achieve a concentration of ≈6M. Subsequent dissolution in 50mM D_2O PBS buffer leads to liquid state polarization of 20%, T1 of 110s and a final concentration of 250mM. For *in vivo* measurements hyperpolarized Cs-BiC solution was injected in the tail vein. Quantification of spatial pH maps was carried out using a GE Signa HDx 3T MRI system with a dual tuned ^{1}H/^{13}C volume coil. Error estimation was performed from error propagation based on the standard deviation of noise of a hyperpolarized BiC spectrum. SPSP pulses with different excitation bandwidths were designed for *in vitro* (72 Hz) and *in vivo* (148 Hz) application. *In vitro* and *in vivo* ^{13}C mapping were performed at a FOV of 8cm and a resolution of 16*16 using SPSP excitation with 20° and 90° flip angles for BiC and CO_2, respectively. FOV was masked by individual SNR thresholds for BiC and CO_2. IDEAL separation was performed with 0.3ms echo time steps and spiral readout afterwards. pH mapping was performed 5s after BiC injection in healthy male Lewis rats in 5 slices: heart, liver, kidneys, bowel, leg with a slice thickness of 10mm. Acute subcutaneous sterile inflammation was induced with Concanavalin A in the right leg of female buffalo rats[3]. pH and proton images were measured 2h after induction of inflammation.

Results and Discussion: First *in vitro* tests of the method using hyperpolarized Na-BiC and phosphate buffer pH-phantoms showed excellent correlation between the derived pH value and the reference pH (±0.03), obtained by pH electrode. An analysis of the signal dynamics revealed that the correct BiC to CO_2 signal ratio is established after 40 seconds, in the absence of carbonic anhydrase. Error estimation (fig.1) of the SPSP excited spectrum reveals that the range of low pH error (<0.2) is 4.77-7.63 for 20° flip angle for BiC and CO_2. Increased SNR of CO_2 due to 90° excitation led to extension of the range to 4.77-8.11 and is therefore sensitive in the biological relevant pH range (6-8). *In vitro* pH maps at ΔpH=0.2 were also measured over 60 seconds and time stability of the method was quantified and proven (data not shown) and also compared to electrode reference pH. Combining SPSP-spiral acquisition with IDEAL encoding allows the separation of the residual BiC signal from the CO_2 acquisition (fig. 2). Quantification of the pH maps shows negligible impact of the present residual BiC signal. pH mapping of rats after administration of high BiC shows evidence of acute metabolic alkalosis and correlates with reduced breathing rate after injection, which recovered with time (fig. 3). Rats with induced inflammation (n=4) show regions of lower pH at the infected region, as expected (fig. 4).

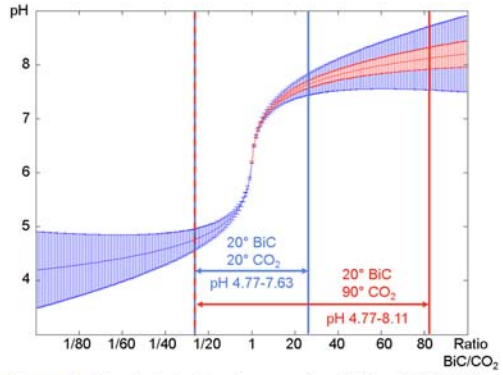

Figure 1: Simulated pH and errors for different BiC/CO_2 ratios. Regions of good pH sensitivity (ΔpH<0.2) for 20° flip angle for BiC and CO_2 (blue) and for 90° CO_2 (red).

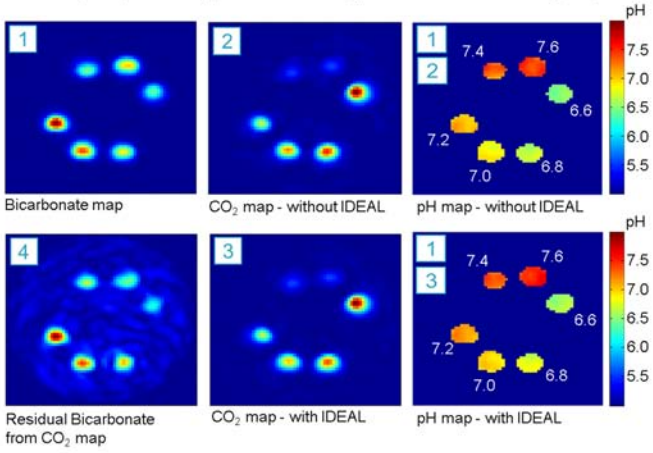

Figure 2: IDEAL separation of the residual BiC signal (4) from SPSP excited spiral acquisition. Top right pH map, based on (1) & (2), was calculated without IDEAL, bottom right pH map, based on (1) & (3), with IDEAL clearing of residual bicarbonate. Both pH maps show excellent correlation of MR values compared to electrode values (white numbers).

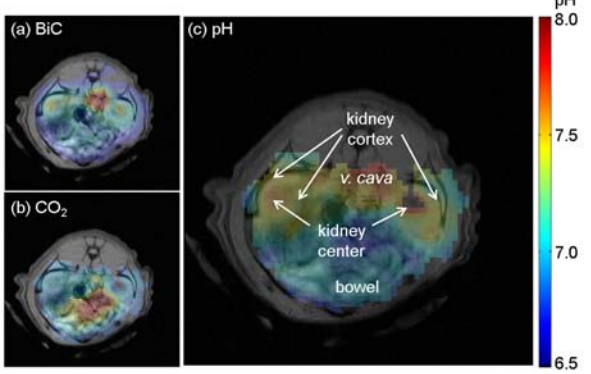

Figure 3: Healthy rat pH map of axial kidney slice. (a): BiC signal. (b): CO_2 signal. BiC occurs mainly in *vena cava* and center of kidneys. CO_2 is mainly in the cortex of the kidneys and the bowel region. (c) Resulting pH map with increased pH of 7.5-7.7 in *vena cava* caused by BiC administration. Bowel region shows low pH around 7. Kidneys show pH gradient from center (pH 7.5) to the cortex (pH 7.2).

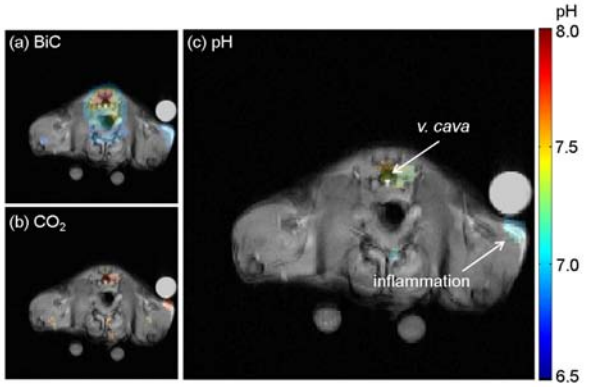

Figure 4: Inflammation induced on right leg of a healthy rat, measured in axial slice. (a): BiC signal. (b): CO_2 signal. BiC concentration is high in the *vena cava* and at the inflamed tissue. Inflammation on GRE proton images is clearly visible and confirmed by histological analysis (data not shown). *V.cava* shows normal blood pH of 7.4. Lower pH of 7.0 at inflamed tissue.

Conclusion and Outlook: Hyperpolarized ^{13}C-BiC pH mapping was shown to be a sensitive method in the biological relevant pH after estimation of physical, chemical and biological uncertancies. It was successfully translated to healthy *in vivo* organ mapping and applied on inflammation and acute metabolic alkalosis models. Further targets could be hypoxia, tumors and inflammation related diseases e.g. Alzheimer disase, Osteoarthritis and Multiple sclerosis.

Acknowledgements:
This work was partly funded by BMBF grant #13EZ1114.
D.J. Scholz acknowledges GSISH for funding

References:
[1] F. A. Gallagher et al., *Nature* 453, no. 7197 (June 12, 2008): 940-943. [2] R. F. Schulte et al., *J Magn Reson*, 2013, 235C, 115-120 [3] I. G. Colditz et al., *Inflammation*, 1987, Vol.11, No.1